Molecular dynamics simulations of the interaction between graphene and lubricating oil molecules

Xianguo Hu (xghu@hfut.edu.cn)
Hefei University of Technology
Feng Qiu
Hefei University of Technology
Hui Song
Hefei University of Technology
Weimin Feng
Hefei University of Technology
Zhiquan Yang
Chinese Academy of Science
Fei Zhang
Hefei University of Technology

Research Article

Keywords: Graphene, Adsorption interaction, Solid-liquid lubrication, Molecular dynamics

Posted Date: November 23rd, 2022

DOI: https://doi.org/10.21203/rs.3.rs-2268673/v1

Molecular dynamics simulations of the interaction between graphene and lubricating oil molecules

Feng Qiu[1], Hui Song[1], Weimin Feng[1], Zhiquan Yang[1,2], Fei Zhang[1], and Xianguo Hu[1,*]

[1]Institute of Tribology, Hefei University of Technology, Hefei 230009, China

[2]State Key Laboratory of Solid Lubrication, Lanzhou Institute of Chemical Physics, Chinese Academy of Science, Lanzhou 730000, China

*Corresponding author. E-mail: xghu@hfut.edu.cn

Abstract

The microscopic interaction between graphene and liquid lubricating oil molecules significantly affects the rheological and tribological properties of the solid-liquid lubricating system. In this study, the interaction between graphene and six kinds of alkane oil droplets with different chain lengths was investigated by molecular dynamics simulations. Interaction energy, atomic concentration distribution, mean square distribution, curvature, centroid, and inclination angle were used to quantitatively describe the effect of interaction differences on lubricating performance. The results demonstrated that with the increase of the carbon chain length, the alkane molecules transformed from a spherical oil droplet model to an ordered layered structure. At the same time, the interaction energy and the angle with the Z coordinate axis were further increased. The self-diffusion movement and the degree of molecular bending were reduced during the interaction, indicating that long-chain alkane molecules interact strongly with graphene, and a dense bilayer adsorption film was formed by horizontal adsorption on the surface of graphene, thus exerting a good lubricating effect. In addition, it was found that the increase in temperature was beneficial to the occurrence of the adsorption process, but high temperature is not conducive to the stable adsorption of alkane molecules on the surface of graphene.

Keywords: Graphene, Adsorption interaction, Solid-liquid lubrication, Molecular dynamics

1 Introduction

Efficient lubrication is one of the most effective ways to reduce energy consumption and carbon dioxide emissions during friction, the use of lubricant avoids direct contact of asperities on the surface of the friction pair, converts dry friction between friction pairs into internal friction between lubricants, thereby reducing friction and wear [1]. However, under extremely variable working conditions with ultra-high loads, a single liquid or solid lubricant cannot exert good tribological properties. For this reason, many scholars have proposed solid-liquid two-phase lubrication, which combined solid lubricants with liquid lubricants. Such as molybdenum disulfide, silicon dioxide, fullerene, graphene, etc. compounded with liquid lubricants, this avoided both cold welding adhesion to solid surfaces and dry friction under transient oil-starved conditions [2-7].

Among them, the excellent mechanical properties of graphene and the weak van der Waals force between layers make it easy to shear slip and have excellent friction reduction properties [8-13], which have attracted extensive attention in the field of tribology. Wu et al. [14,15] added graphene and graphene oxide nanosheets to 4010 aviation lubricating oil and studied the influences of load, rotational speed, etc. on tribological properties. The results showed that the adsorption of the two additives played a role in anti-shear, anti-tear, and filling, avoiding direct contact with the asperities. Ali et al. [16] investigated the tribological properties of graphene-containing lubricating oil through tribometer and bench tests, the results indicated that the addition of graphene improved friction reduction and anti-wear performance, reduced fuel consumption by 17%, and reduced the exhaust gas (CO, CO_2, NO_X) emissions by 2.79-5.42%. Liu et al. [17] dispersed the modified graphene into a base oil, and the modified graphene formed a carbon-containing deposition film on the friction interface to avoid direct contact with the friction pair, thereby improving the tribological performance. Senatore et al. [18] dispersed 0.1% wt graphene oxide (GO) nanosheets into mineral lubricants by ultrasonic technology and found that GO can reduce the friction coefficient (average 20%) in boundary, mixed, elastohydrodynamic lubrication domains, and reduce the wear rate of friction pairs (the wear scare diameter was reduced by 12%, 27%, and 30%, respectively).

However, current research focuses more on the tribological properties and macroscopic

properties exhibited by solid-liquid two-phase lubrication, and less on the micro-level interaction between solid-liquid two-phase lubricants, the interaction difference at the micro level significantly affects the rheological properties, synergistic tribological effects and lubricant mechanism of the lubricant system. Molecular dynamics simulations can investigate micro-level interactions, which is an important complement to experiments [19-25]. Li et al. [26] explored the synergistic lubricant mechanism of graphene water-based lubricant system through molecular dynamics simulations, the results demonstrated that graphene enhanced the movement of water molecules, made it easier to move to the interface, and avoided direct contact of the asperities. Water molecules induced graphene to release lateral stress and played a good role in friction reduction. Zhang et al. [27] studied the interaction between alkane molecules with different chain lengths and palygorskite coatings, it was founded that short-chain alkanes had compatibility with palygorskite, and can stably adsorb on the surface of palygorskite to form a layered lubricating film, which played a good lubricating role. Wu et al. [28] investigated the rheological properties of graphene nanofluids by non-equilibrium molecular dynamics simulations, the results reflected that the addition of graphene increased the viscosity of base oil by 3 times under the conditions of 0.1 MPa, 500K, and has a more important effect on increasing the viscosity of base oil at high temperature and pressure.

The interaction difference at the microscopic level between solid-liquid two-phase lubricants significantly affects the rheological properties, tribological properties, synergistic tribological effects, and lubrication mechanism of the lubricating system. This article aims to investigate the interaction of the solid-liquid two-phase lubrication system of graphene and alkanes with different chain lengths at the microscopic level by molecular dynamics simulations and to reveal the effect of the difference in molecular chain length of alkanes on the lubrication performance. This will provide insights into the compositional differences and base oil use, enabling graphene to exert better tribological properties in solid-liquid two-phase lubrication systems.

2 Models and methods

2.1 Model parameters

All models were established based on Materials Studio (MS) software. Firstly, linear alkane single molecule models with different carbon chain lengths were established, which were n-hexane (C_6H_{14}), n-octane (C_8H_{18}), n-decane ($C_{10}H_{22}$), dodecane ($C_{12}H_{26}$), tetradecane ($C_{14}H_{30}$), and n-docosane ($C_{22}H_{46}$), as shown in Fig. 1a. But the single molecule model cannot simulate a real lubricating system [20]. For this reason, the spherical oil models with a radius of 20 Å were constructed based on the Monte Carlo rule and the real density of each component for later molecular dynamics simulations. The final conformation of the model and the parameters of each component were shown in Fig. 1b and Table 1. Secondly, a lamellar structure with a size of 55.33 Å × 56.19 Å was constructed by supercell processing on the graphene crystal, and the unsaturated dangling bonds at the edge of graphene were functionalized to introduce H atoms to realize the graphene (abbreviated as Gra) model construction [29], as shown in Fig. 1c. Thirdly, the spherical oil droplet model and the lamellar graphene structure were spliced together. To eliminate periodic effects, a vacuum layer of 60 Å was added in the Z direction [27,30]. The size of the simulation system was 60 Å × 60 Å × 100 Å, as shown in Fig. 1d.

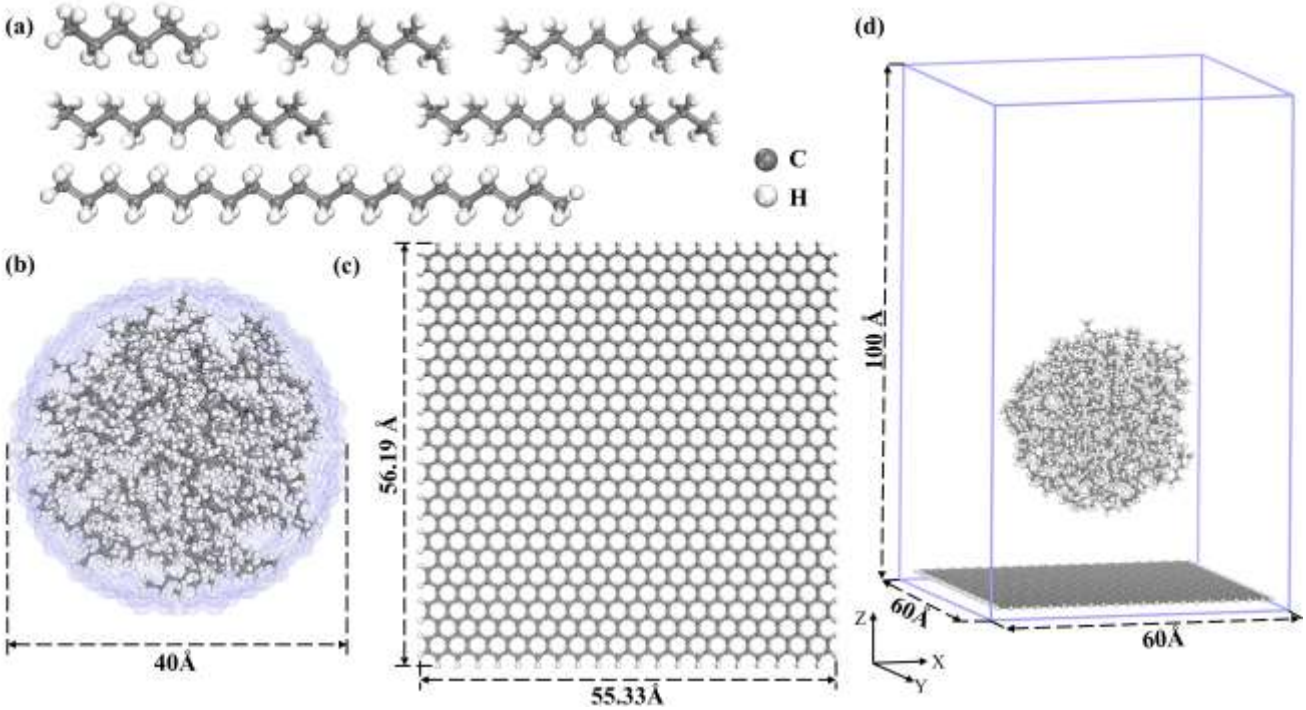

Fig 1 (a) Single-molecule models of alkanes with different chain lengths (**b)** Spherical oil droplet model (**c)** Graphene model (**d)** Lubrication system model

Table 1 Component parameters of spherical oil droplets

Systems	C_6H_{14}	C_8H_{18}	$C_{10}H_{22}$	$C_{12}H_{26}$	$C_{14}H_{30}$	$C_{22}H_{46}$
Oil drop radius (Å)	20	20	20	20	20	20
Density (g/cm^3)	0.660	0.703	0.735	0.753	0.767	0.794
Number of molecules	154	123	103	89	77	51

2.2 Simulation methods

Due to the unreasonable initial configuration, the energy of the system was at a high level. Therefore, geometry optimization and dynamic equilibrium were required to find the low-energy conformation that conforms to the real system [19]. All simulations were done based on the molecular mechanics and molecular dynamics methods of the MS Forcite module, the COMPASS force field suitable for polymer nanocomposite systems were selected [31,32], and the charge of each atom was automatically assigned by the force field parameters.

Step 1 The Smart algorithm was used to geometrically optimize the single molecule models and system models to find the local energy minimum. The energy convergence criterion was 2×10^{-5} kcal/mol, the force convergence criterion was 1×10^{-3} kcal/mol, and the displacement convergence criterion was 1×10^{-5} Å. Step 2 The alkane molecules with different chain lengths were packed into cube boxes and the dynamic simulation of 50000 step annealing and 1000 ps was carried out under the NPT ensemble, as shown in Fig. 2a, b. (The density change curves of other systems were shown in Fig. S1 of the supplementary material.) Fig. 2c shows that the experimental values of density are basically consistent with the calculated values, indicating the rationality of selecting COMPASS force field parameters. Step 3 The dynamic equilibrium of 4000 ps was carried out under the NVT ensemble to eliminate the internal stress and to find a reasonable conformation at the global energy minimum. The temperature was set to room temperature 298.15 K and controlled by the Andersen method [33]. The time step was 1fs, the total number of dynamic simulation steps was 4×10^6 steps, and one frame was output every 1000 steps.

3 Results and discussion

3.1 System equilibrium and conformational evolution

To explore the interaction between the solid-liquid two-phase lubrication system, the energy-temperature curves during the molecular dynamics simulations process and the output configurations of the six systems at four different times were extracted, which were 0 ps, 500 ps, 2000ps, and 4000 ps, respectively, as shown in Fig. 2d and Fig. 3. In Fig. 2d, the temperature of the system fluctuated around the target temperature of 298.15 K during the simulation process, the total energy and each energy component quickly reached equilibrium and fluctuated around the stable value, manifesting that the system has reached a low-energy conformation with reasonable structure, which can be used for subsequent analysis and calculation of relevant properties.

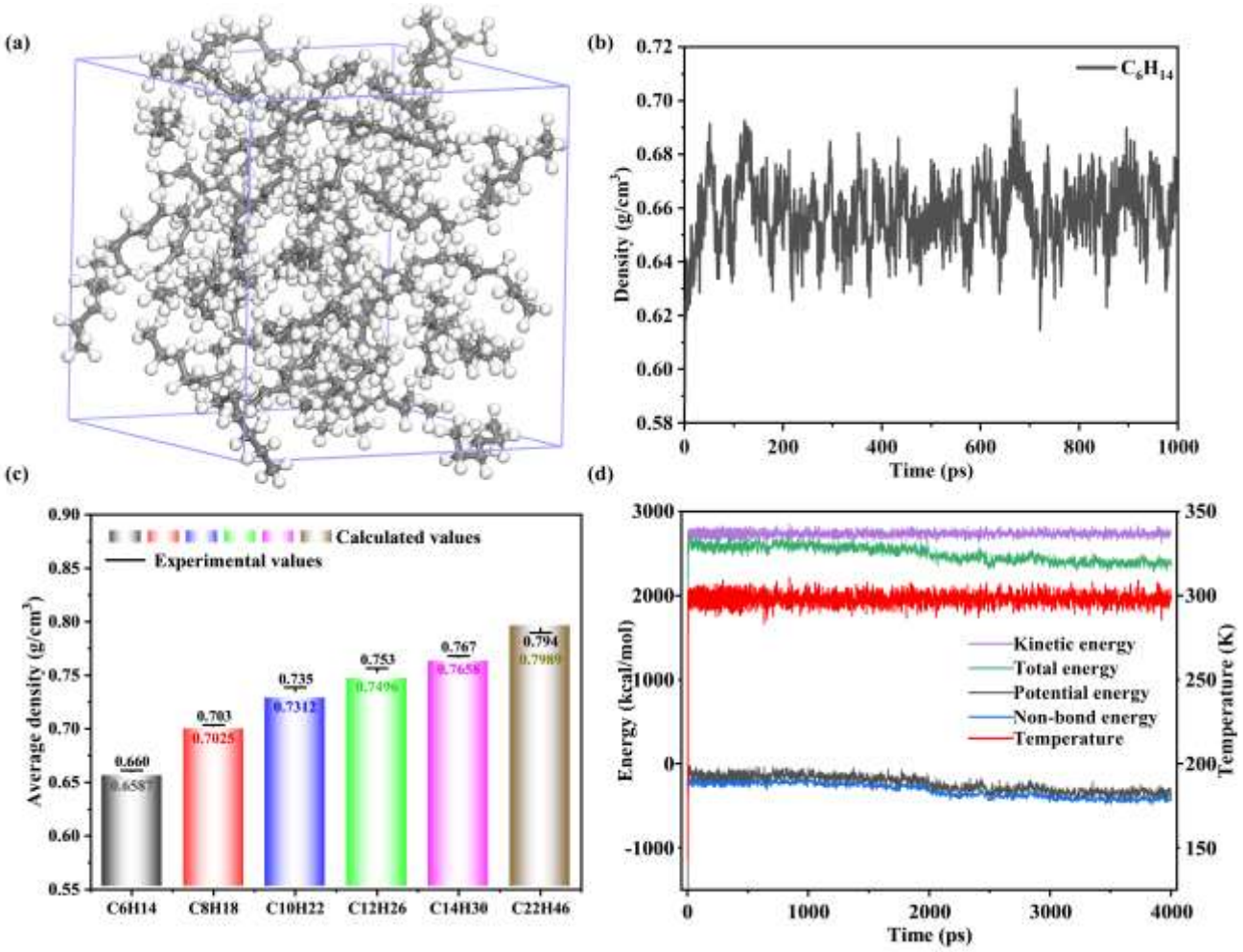

Fig 2 (a) Alkane molecules were packed into cube boxes (**b)** The density change curve of the C_6H_{14} system (**c**)Average density (**d)** Temperature and energy change curves of the system

Based on the system equilibrium, the microstructure evolution during the solid-liquid two-phase interaction at different times was extracted, as shown in Fig. 3. At 0 ps, the layered graphene structure was fixed at the bottom of the box to simulate the solid lubricant during solid-liquid two-phase lubrication. A large number of tribological experiments also confirmed that graphene as a solid lubricant will be adsorbed on the surface of the friction pair to form a stable layered film [16,17]. Models of alkane oil droplets with different chain lengths were placed on the graphene surface with a preset distance of 14 Å to observe the dynamic process of the interaction [27]. After 500 ps dynamics simulation, it is observed from Fig. 3b that alkane oil droplets with different chain lengths show different morphologies. In the Gra/C_6H_{14} system, only a small amount of C_6H_{14} molecules were adsorbed to the surface of graphene, and the overall spherical oil droplet model was still maintained, indicating that the interaction between C_6H_{14} molecules and graphene was weak, and the short-time dynamics process cannot make C_6H_{14} molecules quickly adsorbed on the surface of graphene to form a layered structure. However, with the increase of carbon chain length, in the three systems of Gra/C_8H_{18}/$C_{10}H_{22}$/$C_{12}H_{26}$, it was found that long-chain alkanes formed a dense adsorption monolayer on the surface of graphene, and the spherical oil droplets gradually changed their original shape and transition to a layered oil film during the interaction process. It shows that with the increase in carbon chain length, the interaction between alkane molecules and graphene was enhanced, and it was easier to move to the graphene surface to form stable adsorption at the same time. In the Gra/$C_{14}H_{30}$/$C_{22}H_{46}$ system, no obvious monolayer adsorption film was observed, which may be due to the strong interaction between the $C_{14}H_{30}$/$C_{22}H_{46}$ alkane molecules themselves inhibited the adsorption with graphene, and this will be analyzed in the subsequent analysis. At 2000 ps and 4000 ps, compared with the long-chain alkane system, the Gra/C_6H_{14} system still maintained its original morphology and formed monolayer adsorption, while the other five systems formed a dense double-layer adsorption film. The above conformational evolution shows that with the increase of carbon chain length, the interaction between alkane molecules and graphene was enhanced, and the long-chain alkane molecules are more likely to form an ordered layered oil film on the surface of graphene during the simulation process.

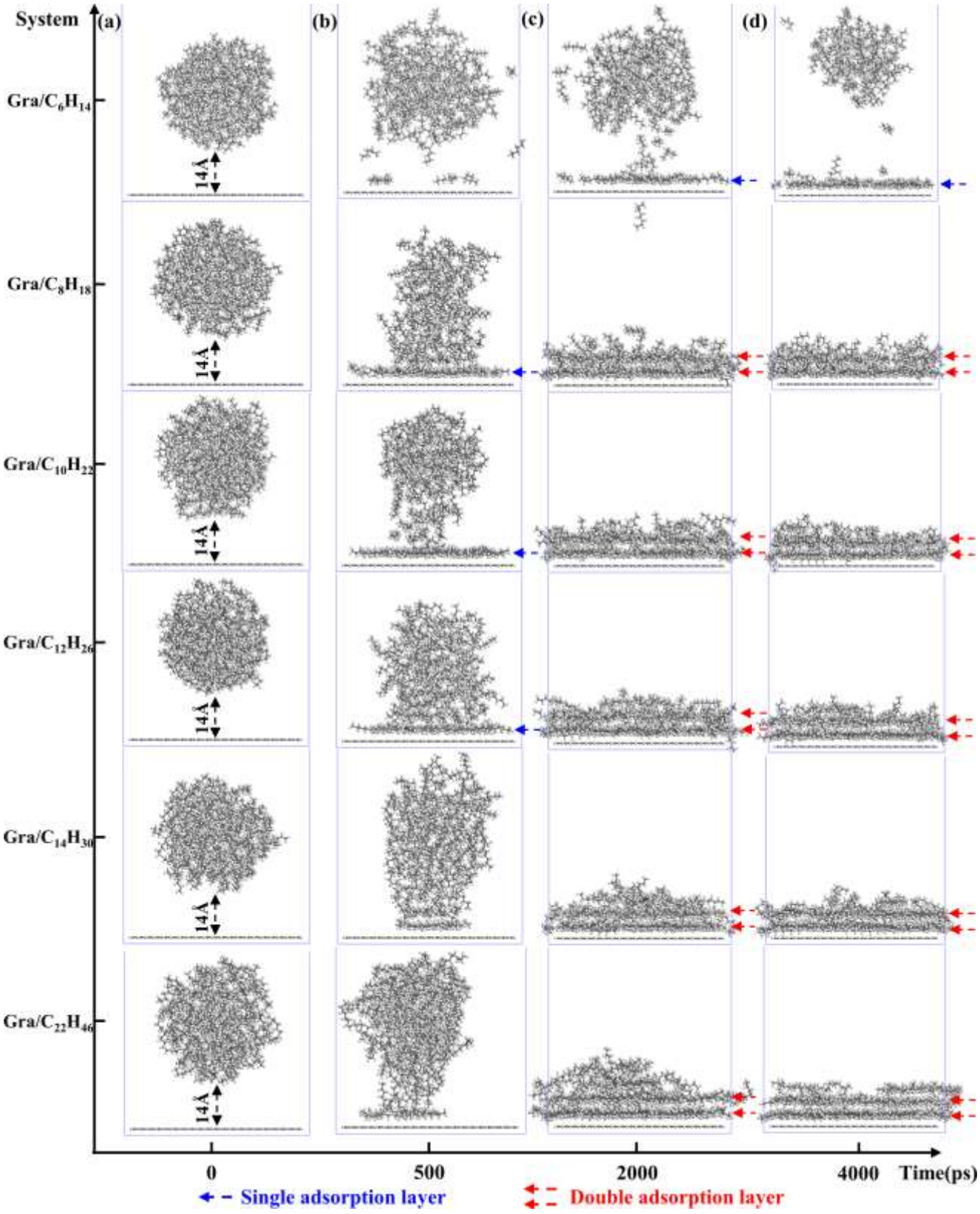

Fig 3 Conformation of solid-liquid two-phase lubrication system at different times

3.2 Interaction energy

To study the reasons for the obvious differences in the structural evolution of the alkane systems with different chain lengths interacting with the graphene surface, the energy changes of each system during the dynamics process were calculated. The adsorption energy between alkanes and graphene and the cohesive energy between alkane molecules are calculated by Eqs. (1) and (2)[34]:

$$E_{adsorption} = E_{total} - (E_{graphene} + E_{alkane}) \quad (1)$$

$$E_{cohesive} = E_{total} - E_{intramolecular} \quad (2)$$

where $E_{adsorption}$ is the adsorption energy between the alkanes and graphene. E_{total}, $E_{graphene}$, and E_{alkane} are the total energy of the system, the energy of graphene alone, the energy of the alkanes system alone, and the energy of the alkanes system alone, respectively. $E_{cohesive}$ is the cohesive energy between alkane molecules, and $E_{intramolecular}$ is the internal energy of the alkanes system. The adsorption energy and cohesive energy are calculated based on the above formulas as shown in Fig. 4a, b.

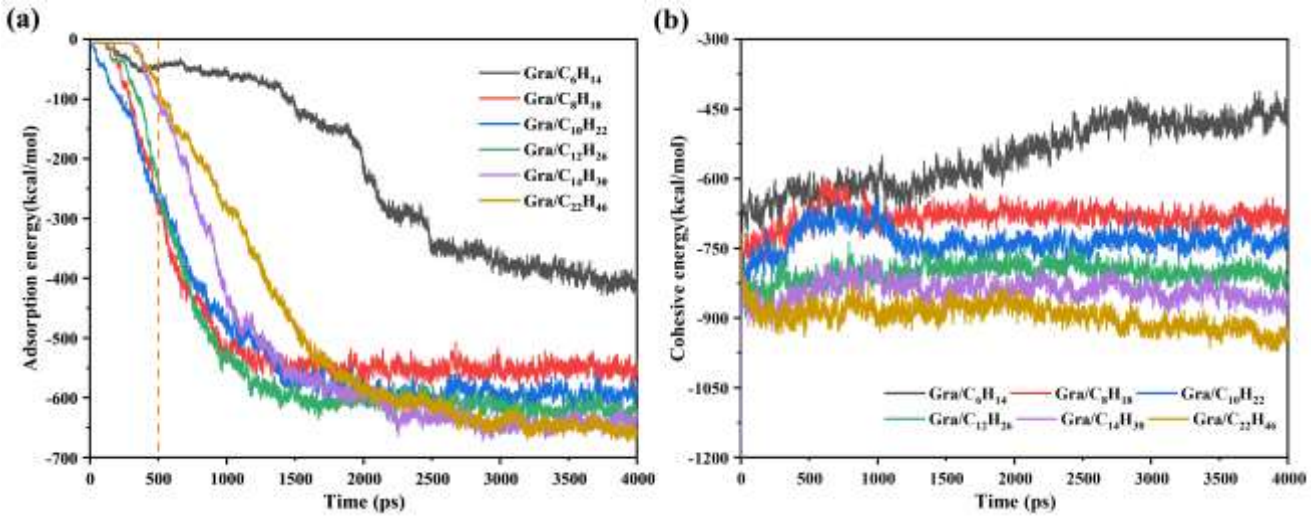

Fig 4 Energy curves between alkanes system and graphene at preset distance 14 Å **(a)** Adsorption energy (**b)** Cohesive energy

According to the principle of thermodynamics, adsorption is an exothermic process, and energy is negative. The larger absolute value of the adsorption energy indicates the stronger adsorption between the alkanes system and graphene, and the formed adsorption film is more

stable [35]. It can be seen from Fig. 4a that the adsorption energy of different systems gradually decreased during the first 500 ps of dynamics simulation, showing that alkane molecules are adsorbing on the graphene surface. Moreover, the absolute value of the adsorption energy of the Gra/C_8H_{18}/$C_{10}H_{22}$/$C_{12}H_{26}$ system is larger than Gra/C_6H_{14} system at 500 ps, indicating that the interaction between long-chain alkanes and graphene is stronger, and short-chain alkanes are weak. However, the adsorption energy of the Gra/$C_{14}H_{30}$/$C_{22}H_{46}$ system does not further increase with the increase of carbon chain length. The reasons for this will be further analyzed by the adsorption energy components and cohesive energy. In subsequent 3500 ps simulations, the adsorption energy of all the systems further decreased and tended to be stable, which is consistent with the adsorption film structure formed in Fig. 3c, d. At the same time, the adsorption energy in the final increases with the increase of carbon chain length, indicating that the longer the molecular chain is, the more stable the adsorption film will be. Why the adsorption energy does not further increase with the increase of carbon chain length at 500ps? To further discuss the reasons for the above differences, the average van der Waals (vdW) and electrostatic interaction were calculated, as shown in Table 2.

Table 2 The average van der Waals energy and electrostatic energy of the system

Energy(kcal/mol)	Gra/C_6H_{14}	Gra/C_8H_{18}	Gra/$C_{10}H_{22}$	Gra/$C_{12}H_{26}$	Gra/$C_{14}H_{30}$	Gra/$C_{22}H_{46}$
Van der Waals	-209.7489	-470.0623	-491.4712	-509.1251	-482.7882	-450.4370
Electrostatic	0.0471	0.0085	0.0708	0.0315	0.0883	0.1447

On the one hand, the adsorption energy is contributed by van der Waals energy and electrostatic energy [36]. It can be seen from Table 2 that the adsorption energy of each system mainly comes from the vdW interaction, and the electrostatic interaction can be ignored, which is due to the weak polarity of linear alkanes, resulting in less electrostatic interaction. The vdW energy is related to the interaction site [37]. The more interaction sites between alkane molecules and the graphene surface, the greater the vdW energy. On the other hand, the interaction between the alkanes system and graphene is not only affected by the adsorption, but also by the interaction between the alkane molecules themselves. Cohesive energy is a parameter to measure the force between substances, which can effectively reflect the bonding

strength of the system. From Fig. 4b we can see that the cohesive energy of each alkanes system changes relatively little during the dynamics simulation process beside Gra/C_6H_{14} system, and the absolute value of the cohesive energy increases with the increase of the carbon chain length. It shows that the longer the alkane chain is, the stronger the bonding between the alkane molecules is, and it is more difficult to interact with graphene during the simulation process, resulting in the Gra/$C_{14}H_{30}$/$C_{22}H_{46}$ system in Fig. 3b not forming a dense monolayer adsorption film. The absolute value of the average energy and energy difference was further calculated, as shown in Fig. 5. We can find from Fig. 5a, and b that the adsorption energy of different chain length alkane systems and graphene are all smaller than the cohesive energy between alkane molecules, indicating that it is difficult for alkane molecules to overcome their interactions in a short time and stably adsorb on the graphene surface. In Fig. 5c, The energy difference of the Gra/C_6H_{14}/$C_{14}H_{30}$/$C_{22}H_{46}$ system is larger than the Gra/C_8H_{18}/$C_{10}H_{22}$/$C_{12}H_{26}$ system, which shows that the adsorption process in the Gra/C_6H_{14}/$C_{14}H_{30}$/$C_{22}H_{46}$ system is more difficult to occur, which is consistent with the structural evolution of Fig. 3b and the adsorption energy change of Fig. 4a, reasonable explanation for the obvious differences in the structural evolution of alkane systems with different chain lengths when interacting with the graphene surface.

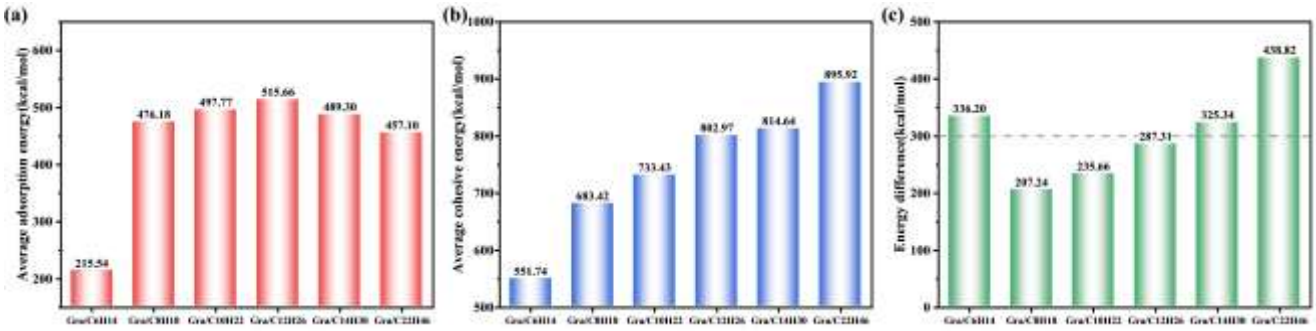

Fig 5 (**a)** Average adsorption energy (**b)** Average cohesive energy (**c)** The energy difference

3.3 Mean square displacement and centroid distance

In molecular dynamics simulations, the diffusion coefficient (D) is often used to evaluate the dynamic behavior of molecules in the system. The larger the diffusion coefficient, the stronger the molecular movement ability. It needs to be obtained by linearly fitting the mean square displacement (MSD) curve according to the Einstein equation. The specific calculation

formula is as follows [26,28].

$$\mathrm{MSD} = \langle |\mathrm{r}(t) - \mathrm{r}(0)|^2 \rangle = \frac{1}{n}\sum_{i=1}^{n} |\mathrm{r_i}(t + t_0) - \mathrm{r_i}(t_0)|^2 \quad (3)$$

$$D = \lim_{t\to\infty} \frac{1}{6t} \langle |\mathrm{r}(t) - \mathrm{r}(0)|^2 \rangle \quad (4)$$

where n represents the total number of atoms, $\mathrm{r_i}(t + t_0)$ and $\mathrm{r_i}(t_0)$ represent the position of the i particle at time $t + t_0$ and t_0, respectively. In order to accurately evaluate the movement ability of alkane systems with different chain lengths, the MSD of 200 ps, 700 ps, and 900 ps in the three stages and centroid distance during the simulations were extracted, and one-sixth of the slope of the MSD linear fitting represents D, as shown in Fig. 6, (Detailed liner equations were shown in Tables S1 – S3 in the supplymentary material). According to Fig. 6a and Table S1, the slope of the first 200ps fitting line decreases with the increase of alkane chain length, indicating that the carbon chain length significantly affects the movement ability of alkane molecules, and the diffusion coefficient decreases with the increase of alkane chain length. This phenomenon was also found in the study of Zhang et al. [27] that the movement ability of alkane molecules weakened with the increase of carbon chain length. Combined with the above energy changes and difference in molecular weight, this may be due to the fact that long-chain alkanes with a large molecular weight are more likely to adsorb on the surface of graphene to form a lubricating film, the attraction of graphene to long-chain alkane molecules inhibits its own diffusion, resulting in a relatively low diffusion coefficient. Therefore, graphene has a weak attraction to short-chain alkane C_6H_{14}, resulting in a relatively high diffusion coefficient, which shows a trend of decreasing diffusion coefficient with the increase of alkane chain length. In the subsequent 700 ps of Fig. 6b, the movement ability of alkane molecules still maintains this rule. The greater MSD of Gra/$C_{14}H_{30}$/$C_{22}H_{46}$ than Gra/$C_{12}H_{26}$ can be attributed to the energy difference is large, which makes it difficult to stable adsorb on the surface of graphene quickly. It can be confirmed by the change of centroid distance in Fig. 6e in the second stage. Combined with the energy change at 500 – 2000 ps in Fig. 4a, the adsorption energy is further reduced, the alkane molecules continue to adsorb with graphene, and we can see that from Fig. 3b, c the alkane molecules transition to an ordered layered structure, from a single-layer adsorption film to a double-layer adsorption film. But in the final 900ps of the third stage,

shown in Fig. 6c, compared with the initial 200ps and subsequent 700 ps, the diffusion coefficients of each system decreased to varying degrees, indicating that the movement ability of alkane molecules was relatively weakened over time. The strong interaction of the graphene surface with alkane molecules further inhibited the movement of alkane molecules, and finally a dense double-layer adsorption film was formed in the Gra/C_8H_{18}/$C_{10}H_{22}$/$C_{12}H_{26}$/$C_{14}H_{30}$/$C_{22}H_{46}$ system, while Gra/C_6H_{14} system formed a single-layer adsorption film, showing a tendency for the diffusion coefficient to decrease with time.

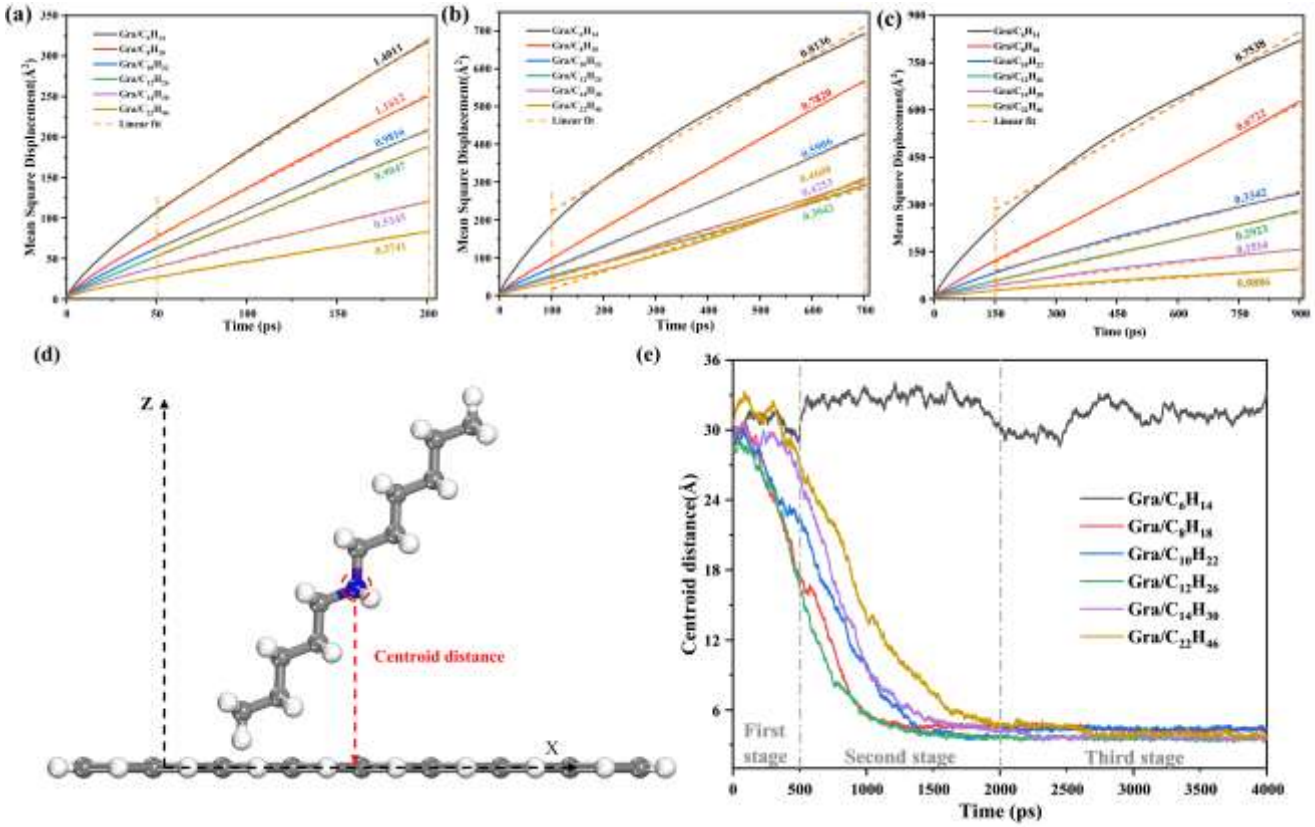

Fig 6 MSD curves of alkane systems with different chain lengths **(a)** Initial 200 ps **(b)** Subsequent 700 ps **(c)** Final 2000 ps **(d)** Schematic diagram of centroid distance **(e)** Distance change between the centroid of the alkane molecules and the XY plane

3.4 Curvature and inclination

According to the conformational evolution of each system at different times in Fig. 3, it can be observed that some alkane molecules transform from the initial spherical oil droplet model to the layered ordered structure. For this reason, the changes in the microstructure were further

studied through the curvature χ and inclination angle θ of the alkane molecules. The curvature χ is defined as the change in the relative distance between the first and last carbon atoms, which reflects the bending degree of alkane molecules. The calculation formula is as follows.

$$\chi = \frac{L - L_0}{L_0} \tag{5}$$

Here χ represents the curvature of alkane molecules, L is the distance between the first and last carbon atoms of the alkane molecules at any time, and L_0 is the distance between the first and last carbon atoms when the alkane molecules are free to stretch, as shown in Fig. 7a. The inclination θ is defined as the angle between the alkane molecules and coordinate axes of X, Y, and Z, as shown in Fig. 7b.

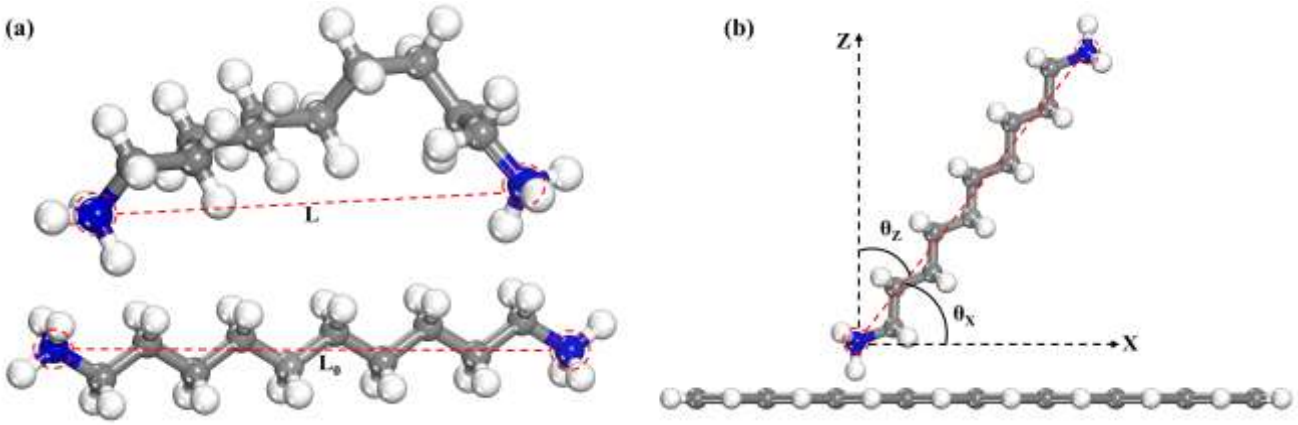

Fig 7 (a) Schematic diagram of curvature and **(b)** inclination angle

Based on the above definitions, the curvature of alkane molecules at different time intervals during the dynamics process was calculated, as shown in Fig. 8, which is the result of statistical averaging of all the molecules in the system. The curvature is less than 0, indicating that the alkane molecules are relatively curved, while the curvature is close to 0, indicating that the alkane molecules are free to stretch. It can be seen from Fig. 8a that during the initial 500ps dynamics simulations, the alkane systems with different carbon chain lengths have a peak near 0, and the intensity of the peaks decreases with the increase of alkane chain lengths, $C_{14}H_{30}$ /$C_{22}H_{46}$ has no peaks near the curvature of 0. This shows that most short-chain alkanes are relatively stretched, while long-chain alkanes are relatively curved. With the increase of alkanes chain length, the degree of bending of alkane molecules increases. In addition, it can also be

found that with the increase of alkane chain length, the number of peaks in each system decreases in turn. It shows that the short-chain alkane molecules are in the form of mostly stretching and few bending, while the long-chain alkanes are on the contrary. And when the carbon chain length continues to increase to the $C_{14}H_{30}/C_{22}H_{46}$, all alkane molecules are in a bent state. During the subsequent 3500ps dynamics simulations, as shown in Fig. 8b, c, the curvature of the C_6H_{14} system remained unchanged, which means that the C_6H_{14} alkane molecules have strong rigidity and still maintain the original shape during the dynamics process. However, the Gra/$C_8H_{18}/C_{10}H_{22}/C_{12}H_{26}/C_{14}H_{30}/C_{22}H_{46}$ system has a trend of increasing the peak value near 0, decreasing the peak value below 0 and shifting the peak value to the right. This indicates that the alkane molecules in the system are further stretched during the simulation, and the distance between the first and last carbon atoms is transitioned from L to L_0, as shown in Fig. 7a.

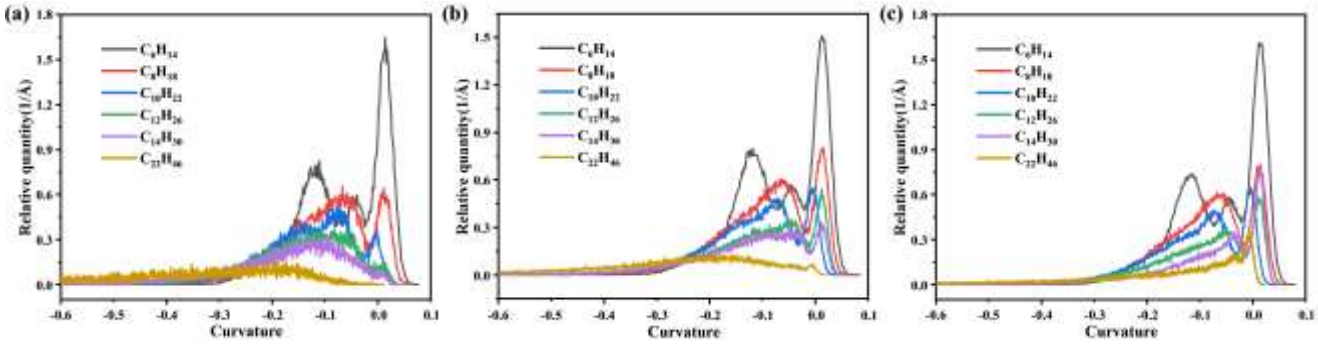

Fig 8 Curvature curve of alkane molecules (**a)** Initial 500 ps (**b)** Subsequent 1500 ps (**c)** Final 2000 ps

The angle between the alkane molecule and the XYZ coordinate axis during dynamics simulations were calculated, and the result of statistical averaging of all the molecules in the system was shown in Fig. 9. The angle between the C_6H_{14} molecule and XY coordinate axis decreases slightly, and the angle with the Z coordinate axis increases slightly, indicating that most of the molecules in the C_6H_{14} alkane system still retain the original spherical oil droplet shape, and some molecules are adsorbed to the surface. However, it can be found from Fig. 9a, c, as the chain length of the alkanes increases, the inclination angle between alkane systems and the X coordinate axis decreased continuously, and the angle with the Z coordinate axis increased significantly. Besides, the angle between alkane molecules and the Y coordinate axis

has no obvious rule from Fig. 9b, indicating that long-chain alkane molecules tend to be perpendicular to the Z coordinate axis and tilt to the X coordinate axis. Due to the weak adsorption of graphene on short-chain alkane molecules, most C_6H_{14} molecules still retain their original spherical oil droplet shape, the strong adsorption with long-chain alkane molecules makes alkane molecules move to the surface of graphene and tend to be horizontally adsorbed on the surface to form a stable layered film.

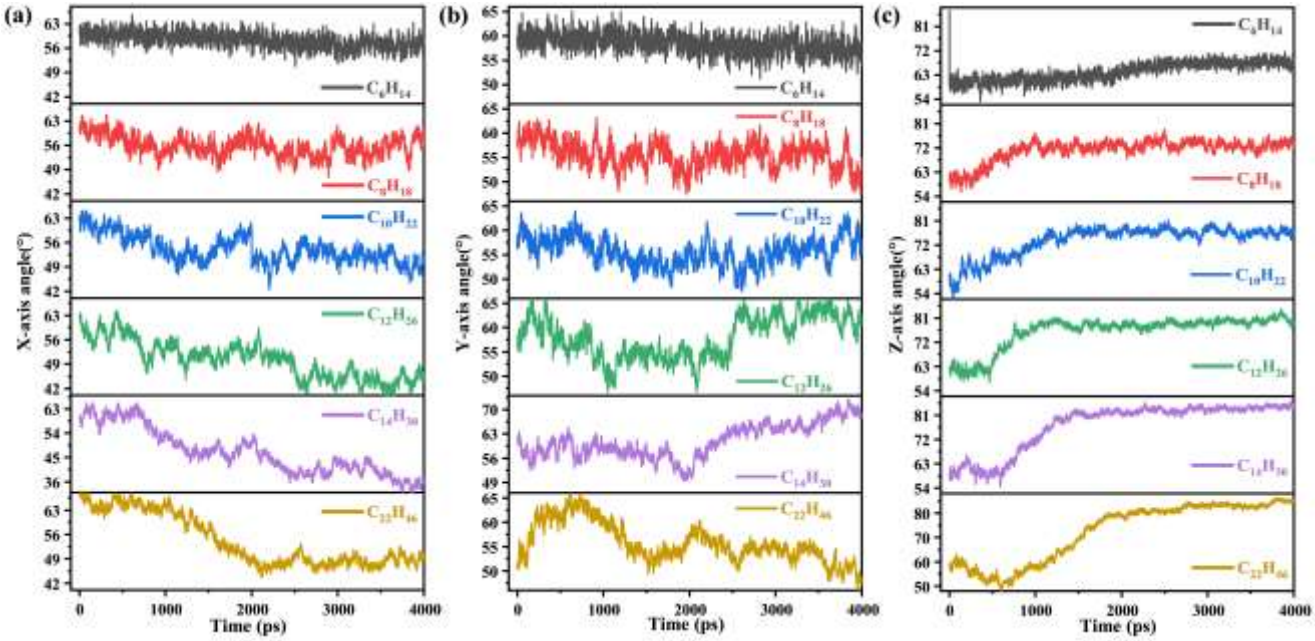

Fig 9 The angle between the alkane molecules and the coordinate axis **(a)** X axis **(b)** Y axis **(c)** Z axis

3.5 Relative atomic concentration

There are obvious differences in the layered adsorption films formed during the interaction. Fig. 10 shows the relative concentration changes along the Z direction for different systems at different times. According to Fig. 10a, the relative concentration curves of different alkane systems have two peaks around 7 Å and 37 Å, respectively, indicating that most of the atoms gather here. Besides, $C_8H_{18}/C_{10}H_{22}/C_{12}H_{26}$ system has higher peaks than $C_6H_{14}/C_{14}H_{30}/C_{22}H_{46}$ system at around 7Å, and the opposite trend appears at 37Å, 7Å corresponds to the centroid position of the first layer of adsorption film, and 37Å corresponds to the centroid position of the alkane oil droplet. It shows that in the first 500 ps simulation process, the alkane molecules

in $C_8H_{18}/C_{10}H_{22}/C_{12}H_{26}$ system are more likely to form a dense monolayer adsorption film on the graphene surface, while in $C_6H_{14}/C_{14}H_{30}/C_{22}H_{46}$ system only a small amount of alkane molecules are adsorbed on the graphene surface to form a loose adsorption film, a large number of alkane molecules are still located at the centroids of the initial alkane oil droplets, as shown in the conformational evolution of Fig. 3b. In Fig. 10b, the peak value of C_6H_{14} near 37 Å decreases, and the peak near 7 Å increases, indicating that the interaction between C_6H_{14} and graphene was enhanced, and the first layer of adsorption film was gradually formed. In the $Gra/C_8H_{18}/C_{10}H_{22}/C_{12}H_{26}/C_{14}H_{30}/C_{22}H_{46}$ system, the peak near 37 Å disappeared, the peak near 7 Å was enhanced, and a new peak appeared near 10 Å, which shows that a dense double-layer adsorption film is further formed based on the single-layer adsorption film. During the final 2000 ps dynamics simulation, we can see from Fig. 10c that the peak near 7 Å and 10 Å was further enhanced and over 16 and 12, respectively. A new peak obviously appeared near 15 Å in $Gra/C_{14}H_{30}/C_{22}H_{46}$ system, it shows that the long-chain alkane system forms a denser adsorption film and exerts a better lubricating effect, which is consistent with the conformational evolution of Fig. 3d.

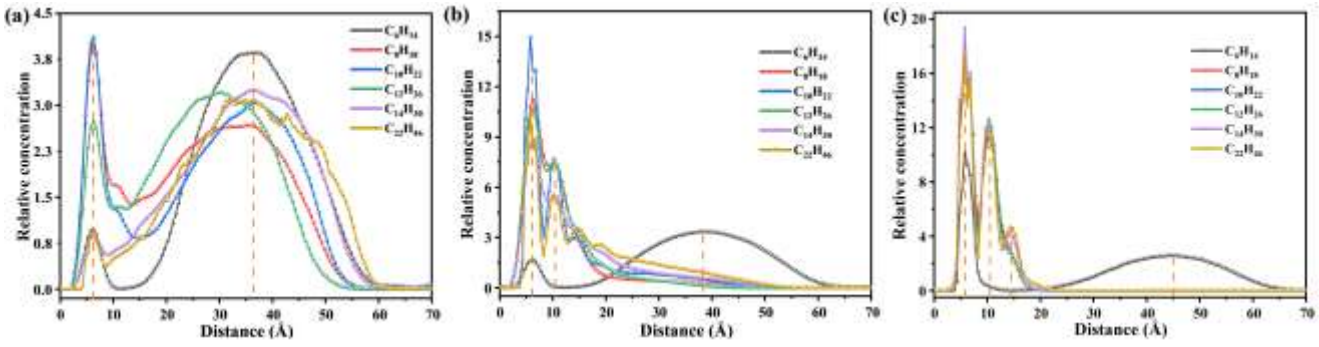

Fig 10 Relative concentration curve of alkane molecules (**a)** Initial 500 ps (**b)** Subsequent 1500 ps (**c**) Final 2000 ps

3.6 Influence of temperature and preset distance

The interaction between alkane molecules and graphene is affected by many factors such as molecule structure, surface morphology, and ambient temperature. The effect of temperature is particularly significant, and Fang et. al. extensively studied the effect of temperature on molecular orientation [38,39]. In this paper, the effects of temperature and preset distance on

the interaction between alkane molecules and graphene were further studied, and the interaction energy of the Gra/C_6H_{14}/$C_{14}H_{30}$/$C_{22}H_{46}$ system during the dynamics simulation was extracted. According to Fig. 11a, for Gra/C_6H_{14} system, the adsorption energy drops sharply with the increase in temperature and tends to be stable. It shows that high temperature is benefit to the occurrence of adsorption process, the increase in temperature increases the thermal motion of molecules and enhances the interaction between alkane molecules and graphene. However, during the last 500 ps, the absolute value of adsorption energy at 400 K is less than 350K, showing a trend that the adsorption energy at a stable period decreases with the increase in temperature. This phenomenon is more obvious in the system of Gra/$C_{14}H_{30}$/$C_{22}H_{46}$, as shown in Fig. 11b, c, the blue curve in the stable stage is higher than the red curve. This suggests that the increase in temperature enhances the thermal movement of molecules, which is benefit to the occurrence of the adsorption process. But it is not conducive to the stable adsorption of alkane molecules on the graphene surface, making the stability of the layered oil film formed on the graphene surface worse.

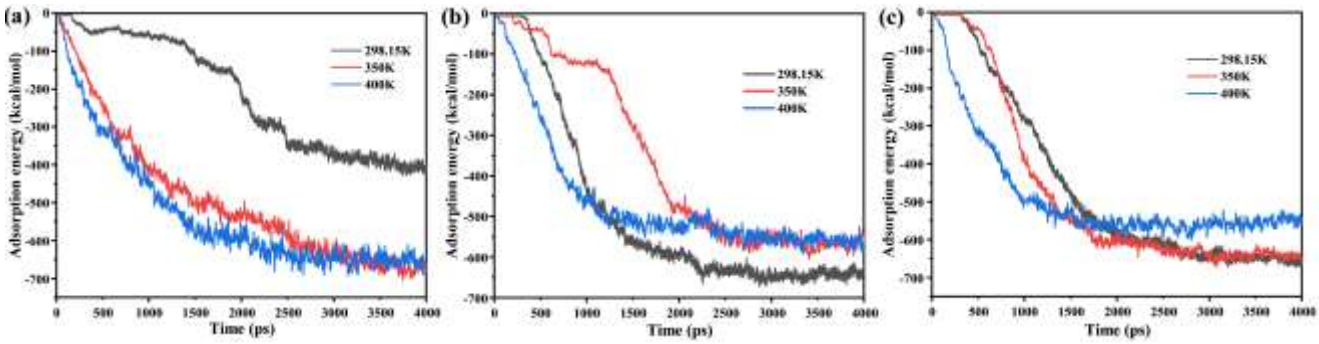

Fig 11 Adsorption energy curves of different systems at different temperatures (**a)** Gra/C_6H_{14} system (**b)** Gra/$C_{14}H_{30}$ system (**c)** Gra/$C_{22}H_{46}$ system

Generally speaking, the actual structure of graphene should be a corrugated surface, there are obvious height differences between the peaks and troughs on the surface. To further explore the influence of surface morphology differences on the interaction, reduced the initial preset distance of the oil droplet from 14 Å to 10 Å to simulate the height difference, and the calculation results in 298.15K are shown in Fig. 12. Compared with Fig. 4a, the reduction of distance makes the adsorption energy of each system drop faster and reach equilibrium quickly,

especially for the Gra/C_6H_{14} system shown in Fig. 12a. This indicates that the decrease of the preset distance between alkane oil droplet and graphene is conducive to the occurrence of interaction so that the alkane molecules can adsorb to the graphene surface faster to form a stable oil film. In addition, compared with Figs.12 and 4 we can see that no matter whether the preset distance is 14 Å or 10 Å, the adsorption energy and cohesive energy at the stable stage increase with the increase of alkane molecular chain length after 4000 ps dynamics simulation. Further confirmed that the interaction between alkane molecules and graphene and the bond strength between alkane molecules was enhanced with the increase of carbon chain length, and the adsorption film formed by long-chain alkanes on the surface of graphene was more stable.

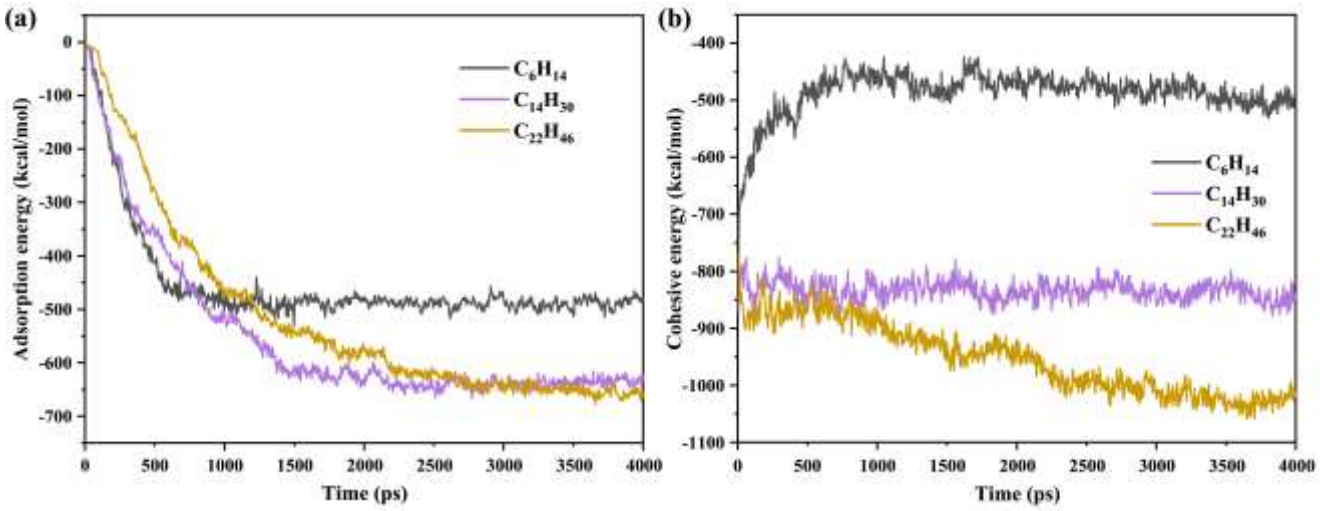

Fig 12 Energy curves of different systems at preset distance 10 Å **(a)** Adsorption energy **(b)** Cohesive energy

4 Conclusions

The interaction difference between graphene and alkane lubricating oil molecules with different chain lengths was investigated by molecular dynamics simulations, which is helpful for the application of graphene as a solid lubricant in a solid-liquid two-phase lubrication system. The result shows that the carbon chain length significantly affects the interaction between alkane molecules and graphene. The interaction energy and the angle with the Z coordinate axis at the stable stage increase with the increase of alkane molecular chain length, and the self-diffusion movement is weakened with the increase of chain length, which is attributed to the strong

attraction of graphene to long-chain alkane molecules inhibiting its self-diffusion motion so that the alkane molecules are horizontally adsorbed on the graphene surface to form a dense double-layer adsorption film, playing a good lubricating effect. Besides, it was found that the increase in temperature and decrease of the distance between alkane oil droplet and graphene was beneficial to the occurrence of adsorption process, but high temperature is not conducive to the stable adsorption of alkane molecules on the surface of graphene.

Acknowledgements

The authors are grateful to the National Nature Science Foundation of China (Grant No. 52075141) for financial support. The authors would also like to thank Dr. Enze Xu from the Hefei University of Technology for his guidance in modeling analysis.

Author contributions

Feng Qiu: Investigation, Formal analysis, Writing-original draft. Hui Song: Methodology, Investigation, Writing-original draft. Weimin Feng: Formal analysis, Visualization, Writing-original draft. Zhiquan Yang: Writing-original draft, Methodology. Fei Zhang: Project administration, Validation. Xianguo Hu: Supervision, Writing-original draft, Validation.

Funding

The authors declare that no funds, grants, or others support were received during the preparation of this manuscript.

Data availability

The raw data can be provided if requested.

Declarations

Conflict of interest The authors declare that they have no conflict of interest.

Consent to participate All authors have read and agreed to the submitted version of the manuscript.

Ethical approval The work is original and has not been published previously or is not under consideration for publication elsewhere.

Supplementary Information Online resources contain supplementary material

References

[1] Ewen JP, Gattinoni C, Morgan N, Spikes HA, Dini D (2016) Nonequilibrium molecular dynamics simulations of organic friction modifiers adsorbed on iron oxide surfaces. Langmuir 32:4450-4463. https://doi.org/10.1021/acs.langmuir.6b00586

[2] Erdemir A, Ramirez G, Eryilmaz OL, Narayanan B, Liao YF, Kamath G, Sankaranarayanan SKRS (2016) Carbon-based tribofilms from lubricating oils. Nature 536:67-71. https://doi.org/10.1038/nature18948

[3] Fan XQ, Xue QJ, Wang LP (2015) Carbon-based solid-liquid lubricating coatings for space applications-A review. Friction 3:191-207. https://doi.org/10.1007/s40544-015-0079-1

[4] Li PP, Ji L, Li HX, Chen L, Liu XH, Zhou HD, Chen JM (2022) Role of nanoparticles in achieving macroscale superlubricity of graphene/nano-SiO_2 particle composites. Friction 10:1305-1316. https://doi.org/10.1007/s40544-021-0532-2

[5] Li XW, Zhang DK, Xu XW, Lee KR (2020) Tailoring the nanostructure of graphene as an oil-based additive: toward synergistic lubrication with an amorphous carbon film. ACS Appl Mater Interfaces 12:43320-43330. https://doi.org/10.1021/acsami.0c12890

[6] Liang HY, Xu MJ, Bu YF, Chen BB, Zhang YH, Fu YH, Xu XJ, Zhang JY(2019) Confined interlayer water enhances solid lubrication performances of graphene oxide films with optimized oxygen functional groups. Appl Surf Sci 485:64-69. https://doi.org/10.1016/j.apsusc.2019.04.190

[7] Toosinezhad A, Alinezhadfar M, Mahdavi S (2020) Tribological behavior of cobalt/graphene composite coatings. Ceram Int 46:16886-16894. https://doi.org/10.1016/j.ceramint.2020.03.267

[8] Li R, Song CG (2018) The influence of hydroxyl groups on friction of graphene at atomic scale. Crystals 8(4):167. https://doi.org/10.3390/ceyst8040167

[9] Li XM, Tao L, Chen ZF, Fang H, Li XS, Wang XR, Xu JB, Zhu HW (2017) Graphene and related two-dimensional materials: structure-property relationships for electronics and optoelectronics. Appl Phys Rev 4:021306. https://doi.org/10.1063/1.4983646

[10] Papageorgiou DG, Kinloch IA, Young RJ (2017) Mechanical properties of graphene and graphene-based nanocomposites. Prog Mater Sci 90:75-127. https://doi.org/10.1016/j.pmatsci.2017.07.004

[11] Soldano C, Mahmood A, Dujardin E (2010) Production, properties and potential of graphene. Carbon 48:2127-2150. https://doi.org/10.1016/j.carbon.2010.02.058

[12] Ye XY, Ma LM, Yang ZG, Wang JQ, Wang HG, Yang SR (2016) Covalent functionalization of fluorinated graphene and subsequent application as water-based lubricant additive. ACS Appl Mater Interfaces 8:7483-7488. https://doi.org/10.1021/acsami.5b10579

[13] Zhu YW, Murali S, Cai WW, Li XS, Suk JW, Potts JR, Ruoff RS (2010) Graphene and graphene oxide: synthesis, properties, and applications. Adv Mater 22:3906-3924. https://doi.org/10.1002/adma.201001068

[14] Wu LP, Gu L, Xie ZJ, Zhang CW, Song BY (2017) Improved tribological properties of Si3N4/GCr15 sliding pairs with few layer graphene as oil additives. Ceram Int 43:14218-14224. https://doi.org/10.1016/j.ceramint.2017.07.168

[15] Wu LP, Xie ZJ, Gu L, Song BY, Wang LQ (2018) Investigation of the tribological behavior of graphene oxide nanoplates as lubricant additives for ceramic/steel contact. Tribol Int 128:113-120. https://doi.org/10.1016/j.triboint.2018.07.027

[16] Ali MKA, Hou XJ, Abdelkareem MAA, Gulzar M, Elsheikh AH (2018) Novel approach of the graphene nanolubricant for energy saving via anti-friction/wear in automobile engines. Tribol Int 124:209-229. https://doi.org/10.1016/j.triboint.2018.04.004

[17] Liu YF, Ge XY, Li JJ (2020) Graphene lubrication. Appl Mater Today 20:100662. https://doi.org/10.1016/j.apmt.2020.100662

[18] Senatore A, D'Agostino V, Petrone V, Ciambelli P, Sarno M (2013) Graphene oxide nanosheets as effective friction modifier for oil lubricant: materials, methods, and tribological results. ISRN Tribol 2013:425809. https://doi.org/10.5402/425809

[19] Ma SJ, Chen P, Xu JL, Xiong XH (2022) Molecular dynamics simulations of key physical properties and microstructure of epoxy resin cured with different curing agents. J Mater Sci 57:1123-1133. https://doi.org/10.1007/s10853-021-06799-w

[20] He JQ, Sun JL, Meng YN, Pei Y, Wu P (2021) Synergistic lubricant effect of Al_2O_3 and MoS_2 nanoparticles confined between iron surfaces: a molecular dynamics study. J Mater Sci 56:9227-9241. https://doi.org/10.1007/s10853-021-05889-z

[21] Song JF, Zhao G (2019) A molecular dynamics study on water lubrication of PTFE sliding against copper. Tribol Int 136:234-239. https://doi.org/10.1016/j.triboint.2019.03.070

[22] Srivastava I, Kotia A, Ghosh SK, Ali MKA (2021) Recent advances of molecular dynamics simulations in nanotribology. J Mol Liq 335:116154. https://doi.org/10/1016/j.moliq.2021.116154

[23] Chen C, Zhang FC, Xu H, Yang ZN, Poletaev GM (2022) Molecular dynamics simulations of dislocation-coherent twin boundary interaction in face-centered cubic metals. J Mater Sci 57:1833-1849. https://doi.org/10.1007/s10853-021-06837-7

[24] Lin DL, Li RY, Li TF, Zi YC, Qi SL, Wu DZ (2021) Effects of pre-imidization on rheological behaviors of polyamic acid solution and thermal mechanical properties of polyimide film: an experiment and molecular dynamics simulation. J Mater Sci 56:14518-14530 https://doi.org/10.1007/s10853-021-06241-1

[25] Zheng X, Su LH, Deng GY, Zhang J, Zhu HT, Anh KT (2021) Study on lubrication characteristics of C4-alkane and nanoparticle during boundary friction by molecular dynamics simulation. Metals 11:1464. https://doi.org/10.3390/met11091464

[26] Li CJ, Tang WW, Tang XZ, Yang LY, Bai LC (2022) A molecular dynamics study on the synergistic lubrication mechanisms of graphene/water-based lubricant systems. Tribol Int 167:107356. https://doi.org/10.1016/j.triboint.2021.107356

[27] Zhang J, Yang L, Wang Y, Wu HC, Cai JB, Xu SS (2021) Molecular dynamics simulation on the interaction between palygorskite coating and linear chain alkane base lubricant. Coatings 11:286. https://doi.org/10.3390/coatings11030286

[28] Wu LP, Keer LM, Lu J, Song BY, Gu L (2018) Molecular dynamics simulations of the rheological properties of graphene-PAO nanofluids. J Mater Sci 53:15969-15976. https://doi.org/10.1007/s10853-018-2756-8

[29] Chawla R, Sharma S (2018) A molecular dynamics study on efficient nanocomposite formation of styrene-butadiene rubber by incorporation of graphene. Graphene Technol 3:25-33. https://doi.org/10.1007/s41127-018-0018-9

[30] Shi JQ, Zhang M, Liu JX, Liu GQ, Zhou F (2021) Molecular dynamics simulations of adsorption

behavior of organic friction modifiers on hydrophilic silica surfaces under the effects of surface coverage and contact pressure. Tribol Int 156:106826. https://doi.org/10.1016/j.triboint.2020.106826

[31] Rigby D, Sun H, Eichinger BE (1997) Computer simulations of poly(ethylene oxide): force field, pvt diagram and cyclization behaviour. Polym Int 44:311-330. https://doi.org/10.1002/(SICI)1097-0126(199711)44:3<311::AID-PI880>3.0.CO;2-H

[32] Sun H (1998) COMPASS: an ab initio force-field optimized for condensed-phase applicationsoverview with details on alkane and benzene compounds. J Phys Chem B 102:7338-7364. https://doi.org/10.1021/jp980939v

[33] Andersen HC (1980) Molecular dynamics simulations at constant pressure and/or temperature. J Chem Phys 72:2384-2393. https://doi.org/10.1063/1.439486

[34] He EQ, Wang SJ, Li YL, Wang Q (2017) Enhanced tribological properties of polymer composites by incorporation of nano-SiO2 particles: a molecular dynamics simulation study. Comput Mater Sci 134:93-99. https://doi.org/10.1016/j.commatsci.2017.03.043

[35] Baseri JR, Palanisamy PN, Sivakumar P (2012) Application of polyaniline nano composite for the adsorption of acid dye from aqueous solutions. E-J Chem 9:1266-1275. https://doi.org/10.1155/2012/415234

[36] Shi JQ, Zhou Q, Sun K, Liu GQ, Zhou F (2020) Understanding adsorption behaviors of organic friction modifiers on hydroxylated SiO2 (001) surfaces: effects of molecular polarity and temperature. Langmuir 36:8543-8553. https://doi.org/10.1021/acs.langmuir.0c01386

[37] Halgren TA (1992) The representation of van der Waals (vdW) interactions in molecular mechanics force fields: potential form, combination rules, and vdW parameters. J Am Chem Soc 114:7827-7843. https://doi.org/10.1021/ja00046a032

[38] LiuYF, Yang H, Zhang ZM, Zhang H (2019) Molecular dynamics simulations on the orientation of n-alkanes with different lengths on graphene. Surf Sci 690:121468. https://doi.org/10.1016/j.susc.2019.121468

[39] Yang H, Liu YF, Zhang H (2018) Fully atomistic molecular dynamics simulations of the isothermal orientation of n-decanes confined between graphene sheets. J Phys Chem C 122:26226-26235 https://doi.org/10.1021/acs.jpcc.8b06191

Supplementary Files

This is a list of supplementary files associated with this preprint. Click to download.

- SupplementaryMaterial.docx